

# Nonrigid Image Registration Using Free-Form Deformations with a Local Rigidity Constraint

Dirk Loeckx, Frederik Maes\*, Dirk Vandermeulen, and Paul Suetens

Medical Image Computing (Radiology–ESAT/PSI), Faculties of Medicine and Engineering, University Hospital Gasthuisberg, Herestraat 49, B-3000 Leuven, Belgium. [Dirk.Loeckx@uz.kuleuven.ac.be](mailto:Dirk.Loeckx@uz.kuleuven.ac.be)

**Abstract.** Voxel-based nonrigid image registration can be formulated as an optimisation problem whose goal is to minimise a cost function, consisting of a first term that characterises the similarity between both images and a second term that regularises the transformation and/or penalties improbable or impossible deformations. Within this paper, we extend previous works on nonrigid image registration by the introduction of a new penalty term that expresses the local rigidity of the deformation. A necessary and sufficient condition for the transformation to be locally rigid at a particular location is that its Jacobian matrix  $J_{\mathbf{T}}$  at this location is orthogonal, satisfying the orthogonality condition  $J_{\mathbf{T}}J_{\mathbf{T}}^T = \mathbf{1}$ . So we define the penalty term as the weighted integral of the Frobenius norm of  $J_{\mathbf{T}}J_{\mathbf{T}}^T - \mathbf{1}$  integrated over the overlap of the images to be registered. We fit the implementation of the penalty term in a multidimensional, continuous and differentiable B-spline deformation framework and analytically determine the derivative of the similarity criterion and the penalty term with respect to the deformation parameters. We show results of the impact of the proposed rigidity constraint on artificial and clinical images demonstrating local shape preservation with the proposed constraint.

## 1 Introduction

Image registration is a common task in medical image processing. The problem of registration arises whenever medical images, e.g. acquired from different scanners, at different time points or pre- and post contrast, need to be combined for analysis or visualisation. For applications where a rigid or affine transformation is appropriate, several fast, robust and accurate algorithms have been reported and validated [1]. However, in many cases the images to be registered show local differences, e.g. due to intra-subject tissue changes over time or inter-subject morphological differences, such that overall affine registration is insufficient and non-rigid image matching is required for accurate local image alignment. Voxel-based nonrigid image registration can be formulated as an optimisation problem

---

\* Frederik Maes is Postdoctoral Fellow of the Fund for Scientific Research - Flanders (FWO-Vlaanderen, Belgium).

whose goal is to minimise a cost function, consisting of a first term that characterises the similarity between both images and a second term that regularises the transformation and/or penalties improbable or impossible deformations. The first term is the driving force behind the registration process and aims to maximise the similarity between the two images. The second term, which is often referred to as the regularisation or penalty term, constrains the transformation between the source and target images to avoid impossible or improbable transformations.

In current literature, the penalty term is often expressed as a global energy term that imposes deformation smoothness by modelling the deforming image as a thin plate [2] or membrane [3]. However, in some applications there is a need to explicitly impose the constraint that some structures in the images to be registered should be treated as rigid objects that do not deform and can only be displaced between both images without changing shape. This is the case for instance with bony structures or contrast-enhancing lesions in intra-subject registration of pre- and post contrast images, e.g. for CT subtraction angiography. Several authors have presented different approaches for incorporating local rigidity constraints in non-rigid image registration. Tanner et al. [4] proposed a solution that locally couples the control points of a B-spline free-form deformation field such as to make the transformation rigid within the specified image region of interest. Little et al. [5] incorporate independent rigid objects in a modified thin-plate spline nonrigid registration. Both approaches require explicit identification of the rigid structures prior to or during registration. Also, they enforce the considered structures to be totally rigid, even in cases where they actually might have deformed slightly. Rohlfing et al. [6] proposed a penalty term that imposes local tissue incompressibility and volume preservation overall in the image without need for segmentation, by constraining the local Jacobian determinant to be close to unity everywhere in the image.

In this paper, we extend the approach of Rohlfing et al. [6] and propose a new penalty term that punishes transformations that are not locally equivalent to a rigid transformation by imposing the local Jacobian matrix to be orthogonal. Local rigidity is controlled by a spatially varying weight factor that depends on tissue type, such that the proposed rigidity constraint can be tuned locally and tailored to the problem at hand.

## 2 Methods

### 2.1 Transformation Model

To register a floating image  $F$  to a reference image  $R$  we need to determine the optimal set of parameters  $\phi_i$  for the transformation  $\mathbf{T}(\Phi) = [T_x, T_y, T_z]$  such that  $F'(\mathbf{x}_r) = F(\mathbf{T}(\mathbf{x}_r; \Phi))$  is in correspondence with  $R$ . For the nonrigid transformation  $\mathbf{T}$ , we use an independent implementation of the B-spline model introduced by Rueckert *et al.* [2]. The transformation model is a multilevel formulation of a free-form deformation based on tensor product B-splines of degree  $d$  (order  $d + 1$ ). Usually,  $d$  is chosen to be 3 for cubic B-splines. The transformation  $\mathbf{T}$  is

defined by a control point grid  $\Phi$ , i.e. a lattice of uniformly spaced control points  $\phi_{i,j,k}$ , where  $-1 \leq i \leq n_x - 1$ ,  $-1 \leq j \leq n_y - 1$ ,  $-1 \leq k \leq n_z - 1$ . The constant spacing between the control points in the  $x$ ,  $y$  and  $z$  direction is denoted by  $\delta_x$ ,  $\delta_y$ ,  $\delta_z$ . At any position  $\mathbf{x} = (x, y, z)$  the deformation is computed from the positions of the surrounding  $(d + 1) \times (d + 1) \times (d + 1)$  neighbourhood of control points

$$\mathbf{T}(\mathbf{x}) = \mathbf{x} + \sum_{l=0}^d \sum_{m=0}^d \sum_{n=0}^d B_l^d(u) B_m^d(v) B_n^d(w) \phi_{i+l, j+m, k+n}. \tag{1}$$

Here,  $i, j$  and  $k$  denote the index of the control point cell containing  $\mathbf{x} = (x, y, z)$ , and  $u, v$  and  $w$  are the relative positions of  $x, y$  and  $z$  inside that cell in three dimensions, e.g.  $i = \lfloor x/\delta_x \rfloor - 1$  and  $u = x/\delta_x - (i + 1)$ . The functions  $B_n^d$  are the B-splines of degree  $d$ . The parameters  $\phi_\iota$  of the transformation  $\mathbf{T}$  are the coordinates of the control points  $\phi_{i,j,k} = \phi_\iota = [\phi_{\iota,x}, \phi_{\iota,y}, \phi_{\iota,z}]$ .

### 2.2 Cost Function

The proposed cost function  $E$  consists of a similarity measure  $E_s$  and a penalty energy  $E_p$ , each weighted with a weight factor

$$E_c = \omega_s E_s + \omega_p E_p. \tag{2}$$

The similarity measure  $E_s$  is the driving force behind the registration process and aims to maximise the similarity between the two images, whereas the penalty term  $E_p$  tries to discourage certain improbable or impossible transformations. The main contribution of this article is the introduction of a new penalty term (and it's derivative) that constrains the transformation between the source and target image to locally rigid transformations.

**Similarity Measure.** We use mutual information of corresponding voxel intensities [7,8] as the similarity measure. To improve the smoothness of the similarity measure and to make the criterion derivable, we construct the joint histogram using Parzen windowing as proposed by Thévenaz *et al.* [9]

$$\forall r \in B_R, f \in B_F :$$

$$p(r, f; \Phi) = \sum_{\mathbf{x}_i \in (R \cap F')} w\left(\frac{f - I_F(\mathbf{T}(\mathbf{x}_i; \Phi))}{\epsilon_f}\right) \cdot w\left(\frac{r - I_R(\mathbf{x}_i)}{\epsilon_r}\right) \tag{3}$$

$$p(f; \Phi) = \sum_{r \in B_R} p(r, f; \Phi), \quad p(r) = \sum_{f \in B_F} p(r, f; \Phi) \tag{4}$$

with  $B_f$  and  $B_r$  the number of bins and using the  $d$ th degree B-spline as window function  $w$ . From the joint histogram, we can calculate the mutual information, which we will use as similarity measure

$$E_s = I(R, F; \Phi) = \sum_{r \in B_R} \sum_{f \in B_F} p(r, f; \Phi) \log \left( \frac{p(r, f; \Phi)}{p(r) \cdot p(f; \Phi)} \right). \tag{5}$$

**Penalty Term.** The main contribution of this paper is the introduction of a local rigidity constraint penalty term, based on the Jacobian matrix. In a small neighbourhood of the point  $\mathbf{x}$ , the non-rigid transformation  $\mathbf{T}$  can be approximated by means of the Jacobian matrix  $J_{\mathbf{T}}(\mathbf{x})$ , which is the local first order or affine approximation to  $\mathbf{T}(\mathbf{x})$ .

$$J_{\mathbf{T}}(\mathbf{x}; \Phi) = \begin{bmatrix} \frac{\partial T_x(\mathbf{x}; \Phi)}{\partial x} & \frac{\partial T_x(\mathbf{x}; \Phi)}{\partial y} & \frac{\partial T_x(\mathbf{x}; \Phi)}{\partial z} \\ \frac{\partial T_y(\mathbf{x}; \Phi)}{\partial x} & \frac{\partial T_y(\mathbf{x}; \Phi)}{\partial y} & \frac{\partial T_y(\mathbf{x}; \Phi)}{\partial z} \\ \frac{\partial T_z(\mathbf{x}; \Phi)}{\partial x} & \frac{\partial T_z(\mathbf{x}; \Phi)}{\partial y} & \frac{\partial T_z(\mathbf{x}; \Phi)}{\partial z} \end{bmatrix} \quad (6)$$

where

$$J_{\mathbf{T}}^T = \begin{bmatrix} \frac{\partial \mathbf{T}}{\partial x} \\ \frac{\partial \mathbf{T}}{\partial y} \\ \frac{\partial \mathbf{T}}{\partial z} \end{bmatrix} = \mathbf{1} + \sum_{l,m,n=0}^d \begin{bmatrix} \frac{1}{\delta_x} \frac{dB_l^d(u)}{du} B_m^d(v) B_n^d(w) \\ \frac{1}{\delta_y} B_l^d(u) \frac{dB_m^d(v)}{dv} B_n^d(w) \\ \frac{1}{\delta_z} B_l^d(u) B_m^d(v) \frac{dB_n^d(w)}{dw} \end{bmatrix} \phi_{i+l,j+m,k+n}. \quad (7)$$

Using the B-spline derivative properties,  $dB^d(u)/du$  can be computed analytically [10] as

$$\frac{dB^d(u)}{du} = B^{d-1}(u + 1/2) - B^{d-1}(u - 1/2). \quad (8)$$

To obtain a locally rigid transformation, a necessary and sufficient condition is that  $J_{\mathbf{T}}$  is an orthogonal matrix, satisfying the orthogonality condition  $J_{\mathbf{T}} J_{\mathbf{T}}^T = \mathbf{1}$ . This condition constrains the deformation to be either a rigid rotation ( $\det(J_{\mathbf{T}}) = 1$ ) or a rotoinversion ( $\det(J_{\mathbf{T}}) = -1$ ). Since both kinds of transformations form separated subsets and as we initiate  $\mathbf{T}$  with the identity matrix, we assume we will not reach any rotoinversion. Therefore, we define the rigidity penalty term as the integral of the Frobenius norm of  $J_{\mathbf{T}} J_{\mathbf{T}}^T - \mathbf{1}$  integrated over the overlap of the reference and the transformed floating image. Alternatively, one could multiply the orthogonality condition with  $\det(J_{\mathbf{T}})$ .

As different structures in the images may have different deformation properties and thus do not need to deform similarly, a local weight term  $w(\mathbf{x})$  is added. This weight can be intensity based, e.g.  $w(\mathbf{x})$  is a function of  $F(\mathbf{T}(\mathbf{x}; \Phi))$ , or based upon a prior segmentation of the floating or reference image. Finally, the total penalty term is given by

$$E_p = \int_{R \cap F'} w(\mathbf{x}) \|J_{\mathbf{T}} J_{\mathbf{T}}^T - \mathbf{1}\|_F d\mathbf{x}. \quad (9)$$

Similar to Rohlfing *et al.* [6], we compute the penalty term as a discrete approximation to the continuous integral calculated over the set of sampled voxels contained in  $R \cap F'$ .

### 2.3 Optimization

We use an optimization method similar to Rueckert *et al.* [2] and Rohlfing *et al.* [6]: the gradient  $\partial E_c / \partial \phi_l = \omega_s \partial E_s / \partial \phi_l + \omega_p \partial E_p / \partial \phi_l$  of the cost function

(2) is computed, and next a simple line search (Van Wijngaarden–Dekker–Brent Method [11]) is performed along the direction of maximal descent. This procedure is repeated until the cost function cannot be improved any further, after which the algorithm continues to a finer resolution (either by refining the deformation mesh or the image resolution).

Instead of using a finite-difference approximation to the derivative like in [6], we perform an analytical calculation of the derivative with respect to the transformation parameters  $\Phi$  (see Thévenaz *et al.* [9] for more details). The derivative of the mutual information is given by

$$\frac{\partial E_s}{\partial \phi_\iota} = \frac{\partial I(R, F; \Phi)}{\partial \phi_\iota} = \sum_{r \in R} \sum_{f \in F} \frac{\partial p(r, f; \Phi)}{\partial \phi_\iota} \cdot \log \left( \frac{p(r, f; \Phi)}{p(f; \Phi)} \right). \tag{10}$$

using the fact that

$$\sum_{r \in R} \sum_{f \in F} \frac{\partial p(r, f; \Phi)}{\partial \phi_\iota} = \sum_{f \in F} \frac{\partial p(f; \Phi)}{\partial \phi_\iota} = 0 \tag{11}$$

The Frobenius norm of the matrix  $A$  is  $\|A\|_F = \sqrt{\sum_{i,j} (A_{i,j})^2}$ , such that the derivative of the penalty term with respect to a deformation parameter is given by

$$\frac{\partial E_p(\mathbf{T})}{\partial \phi_{\iota,\kappa}} = - \int_{R \cap F'} w(\mathbf{x}) \frac{\sum_{i,j} [J_{\mathbf{T}} J_{\mathbf{T}}^T - \mathbf{1}]_{ij} \left[ \frac{\partial J_{\mathbf{T}}}{\partial \phi_{\iota,\kappa}} J_{\mathbf{T}}^T + J_{\mathbf{T}} \frac{\partial J_{\mathbf{T}}^T}{\partial \phi_{\iota,\kappa}} \right]_{ij}}{\|J_{\mathbf{T}} J_{\mathbf{T}}^T - \mathbf{1}\|_F} d\mathbf{x} \tag{12}$$

where

$$\frac{\partial J_{\mathbf{T}}}{\partial \phi_{\iota,\kappa}}{}^T = \begin{bmatrix} \frac{\partial^2 \mathbf{T}}{\partial \phi_{\iota,\kappa} \partial x} \\ \frac{\partial^2 \mathbf{T}}{\partial \phi_{\iota,\kappa} \partial y} \\ \frac{\partial^2 \mathbf{T}}{\partial \phi_{\iota,\kappa} \partial z} \end{bmatrix} = \begin{bmatrix} \frac{1}{\delta_x} \frac{dB_l^d(u)}{du} B_m^d(v) B_n^d(w) \\ \frac{1}{\delta_y} B_l^d(u) \frac{dB_m^d(v)}{dv} B_n^d(w) \\ \frac{1}{\delta_z} B_l^d(u) B_m^d(v) \frac{dB_n^d(w)}{dw} \end{bmatrix} \mathbf{e}_\kappa \tag{13}$$

for  $\kappa = x, y, z$  and with  $\mathbf{e}_\kappa$  the unit vector along coordinate axis  $\kappa$ . We see that the non-zero element of e.g.  $\frac{\partial^2 \mathbf{T}}{\partial \phi_{\iota,\kappa} \partial x}$  is the same over all components of  $\phi_\iota$  and independent of its value, allowing for an efficient precalculation of its values.

### 3 Experiments

To indicate the feasibility and usefulness of the proposed approach, we applied it to three different data sets (figure 1). The first data set consists of artificial images, roughly depicting a vessel containing calcified regions. Although the vessel changes shape between the floating and the reference image, the shape of the calcified regions and bony structures is supposed to remain constant. Therefore, we chose a weight function  $w(\mathbf{x}) = 1$  for high-intense regions and  $w(\mathbf{x}) = 0$  otherwise. As can be seen from the results, the shape of the rigid structures is

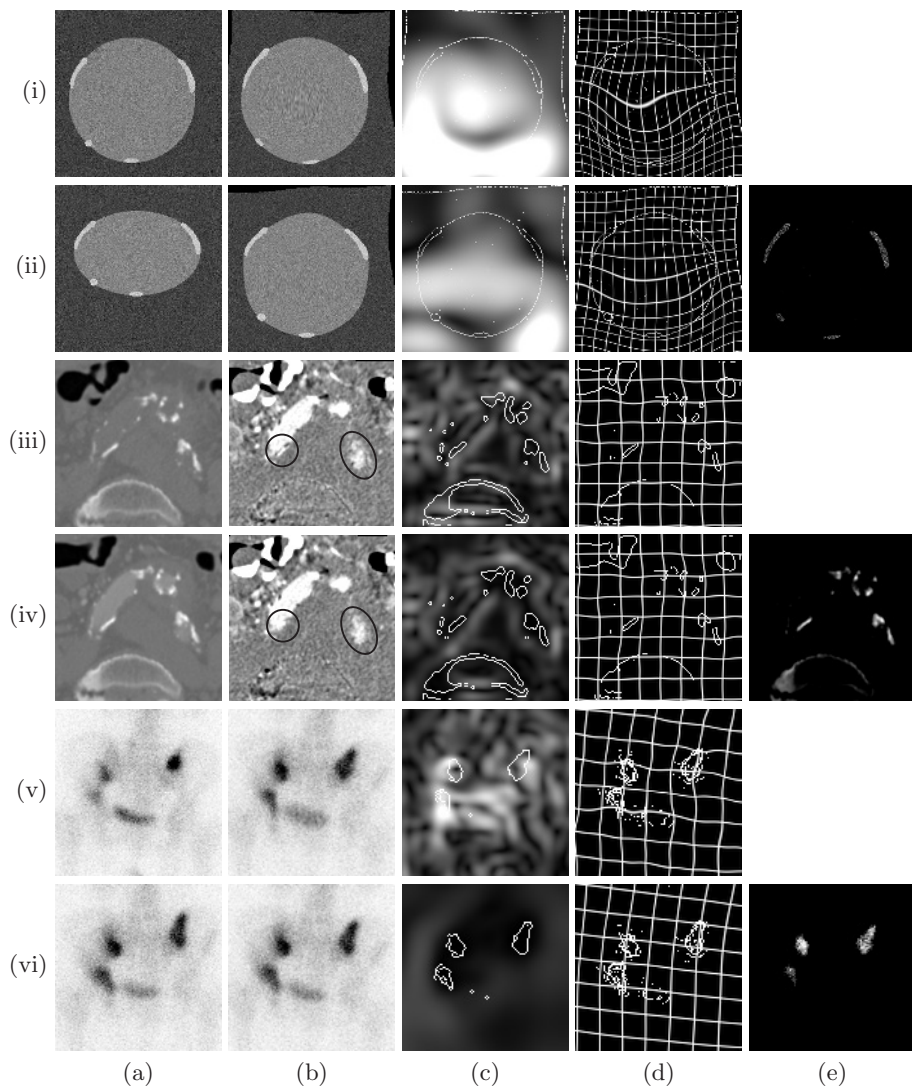


**Fig. 1.** Validation data sets. From top to bottom: artificial CTA slice, detail of clinical CTA slice, detail of clinical PET scan. Rows (i), (iii) and (v) display the reference images and the registration results without the penalty term, rows (ii), (iv) and (vi) display the floating images and the registration results with the penalty term. The columns contain (a) the reference and floating image, (b) the registered images (reference image subtracted from registered floating image in (iii) and (iv)), (c) the unweighted penalty term, (d) the obtained deformation grid, and (e) the local weight function  $w(\mathbf{x})$ . The penalty term and deformation field images are overlaid with the edges of the registered image.

preserved better using the proposed penalty term than without. E.g., the bigger calcifications at the top of the image are more elongated, whereas the smaller calcifications at the bottom are slightly compressed. This is confirmed by the images in column (d), that show a high non-rigidity factor in the unconstrained case, and almost no deformation in the constrained case.

The second example (figure 1, rows (iii) and (iv)) shows a detail of a registered computed tomography angiography (CTA) slice. We chose a weight factor that increases linear with intensity in the high-intense regions, and is zero otherwise. As can be seen in column (c), an unconstrained registration causes local shape deformations in the calcified or bony regions. When we use the approach proposed in this article, the deformation is locally rigid in the selected structures. As expected, this has a positive influence on the artifacts in the difference images (column (b)).

The third data set we applied the algorithm to consists of full body PET images, acquired at different time points during treatment. As we want to study the evolution of the lesion over time, we do not want the non-rigid registration to locally deform it. The results of the registration are shown in figure 1, rows (v-vi). We used a weight function similar to the previous case, preventing the lesions to change shape. Close observation of column (b) shows that in the unconstrained case, the lower left region did slightly shrink while the lower middle lesion did grow.

## 4 Discussion

A new local rigidity penalty term for non-rigid image registration is proposed, modelling the weighted local rigidity of the transformation. This penalty term is useful for the registration of images where certain structures can not or should not change shape. Its applicability is shown on three example data sets.

The introduction of the local weight factor enables the deformation to preserve the shape in selected regions while still allowing the deformation to non-rigidly align both images. The determination of the weight factor necessitates some kind of segmentation, labelled or statistical, of at least one of the images. Several approaches for this segmentation are possible, ranging from simple intensity thresholding as in the samples shown here, over the use of a more advanced segmentation algorithm like e.g. level-set segmentation, to a joint segmentation/registration approach, where in each iteration the segmentation is updated based on the current registration and vice versa.

In future research, we will validate our registration method on different kinds of images in two and three dimensions, investigate the influence of the weight factors and compare the rigidity constraint with other constraints, especially the volume preserving constraint introduced by Rohlfing *et al.* [6]. However, because usually no ground truth exists giving the correct deformation field, the validation of nonrigid registration algorithms is difficult and an active area of research. A promising validation method was recently introduced by Schnabel *et al.* [12], using a biomechanical model to simulate non-rigid deformations.

**Acknowledgements** This work is part of K.U.Leuven/OF/GOA/1999/05, K.U.Leuven/OF/GOA/2004/05 and FWO G.0258.02.

## References

1. West, J., Fitzpatrick, J.M., Wang, M.Y., Dawant, B.M., Maurer, Jr., C.R., Kessler, R.M., Maciunas, R.J., Barillot, C., Lemoine, D., Collignon, A., Maes, F., Suetens, P., Vandermeulen, D., van den Elsen, P.A., Napel, S., Sumanaweera, T.S., Harkness, B., Hemler, P.F., Hill, D.L.G., Hawkes, D.J., Studholme, C., Maintz, J.B.A., Viergever, M.A., Malandain, G., Pennec, X., Noz, M.E., Maguire, Jr., G.Q., Pollock, M., Pelizzari, C.A., Robb, R.A., Hanson, D., Woods, R.P.: Comparison and evaluation of retrospective intermodality brain image registration techniques. *Journal of Computer Assisted Tomography* **21** (1997) 554–566
2. Rueckert, D., Sonoda, L.I., Hayes, C., Hill, D.L.G., Leach, M.O., Hawkes, D.J.: Nonrigid registration using free-form deformations: Application to breast MR images. *IEEE Trans. Med. Imag.* **18** (1999) 712–721
3. Amit, Y., Grenander, U., Piccioni, M.: Structural image restoration through deformable templates. *J. Amer. Statist. Assoc.* **86** (1991) 376–387
4. Tanner, C., Schnabel, J.A., Chung, D., Clarkson, M.J., Rueckert, D., Hill, D.L.G., Hawkes, D.J.: Volume and shape preservation of enhancing lesions when applying non-rigid registration to a time series of contrast enhancing MR breast images. In Delp, S.L., DiGioia, A.M., Jaramaz, B., eds.: *Medical Image Computing and Computer-Assisted Intervention (MICCAI 2000)*. Volume 1935 of *Lecture Notes in Computer Science.*, Springer Verlag (2000) 327–337
5. Little, J.A., Hill, D.L.G., Hawkes, D.J.: Deformations incorporating rigid structures. *Comput. Vis. Image Underst.* **66** (1997) 223–232
6. Rohlfing, T., C.R. Maurer, J., Bluemke, D., Jacobs, M.: Volume-preserving non-rigid registration of MR breast images using free-form deformation with an incompressibility constraint. *IEEE Trans. Med. Imag.* **22** (2003) 730–741
7. Maes, F., Collignon, A., Vandermeulen, D., Marchal, G., Suetens, P.: Multimodality image registration by maximization of mutual information. *IEEE Trans. Med. Imag.* **16** (1997) 187–198
8. Viola, P., Wells, W.: Alignment by maximization of mutual information. *International Journal of Computer Vision* **24** (1997) 137–154
9. Thévenaz, P., Unser, M.: Optimization of mutual information for multiresolution image registration. *IEEE Trans. Med. Imag.* **9** (2000) 2083–2099
10. Unser, M.: Splines: A perfect fit for signal and image processing. *IEEE Signal Processing Mag.* **16** (1999) 22–38
11. Press, W.H., Teukolsky, S.A., Vetterling, W.T., Flannery, B.P.: *Numerical Recipes in C: The Art of Scientific Computing*. Cambridge University Press (1992)
12. Schnabel, J.A., Tanner, C., Castellano-Smith, A.D., Leach, M.O., Hayes, C., Degenhard, A., Hose, R., Hill, D.L.G., Hawkes, D.J.: Validation of non-rigid registration using finite element methods. In Insana, M.F., Leahy, R.M., eds.: *XVIIth International Conference on Information Processing in Medical Imaging (IPMI'01)*. Volume 2082 of *Lecture Notes in Computer Science.*, Springer Verlag (2001) 344–357